



Optimizing Power Factor in SixGe_{1-x} Alloys and Some Other Thermoelectric Materials: Insights and Empirical Relationships

Irakli Nakhutsrishvili ^{a*} and Zurab Adamia ^b

^a *Institute of Cybernetics, Georgian Technical University, Tbilisi, Georgia.*

^b *Sukhumi State University, Georgia.*

Authors' contributions

This work was carried out in collaboration between both authors. Both authors read and approved the final manuscript.

Article Information

Open Peer Review History:

This journal follows the Advanced Open Peer Review policy. Identity of the Reviewers, Editor(s) and additional Reviewers, peer review comments, different versions of the manuscript, comments of the editors, etc are available here: <https://www.sdiarticle5.com/review-history/116184>

Received: 23/02/2024

Accepted: 27/04/2024

Published: 01/05/2024

Short Communication

ABSTRACT

In this article, the issue of determining the power factor maximums of Si_xGe_{1-x} alloy with different compositions is investigated. This issue is discussed also for other thermoelectrics based on literature data. It is shown that for the values of the Seebeck coefficient in the interval (1-4)10⁻⁴V/K, (PF)_{max} corresponds to the minimum of the specific electrical conductivity. The interdependence of these thermoelectric parameters has a regular character. The dependences lg(σS²)_{max} – lgσ_{min} for various thermoelectrics based on literature and our data in the corresponding interval of changes of variables are described by a single empirical expression lg(σS²)_{max} ≅ 0.583(lgσ_{min})² - 3.332lgσ_{min}. The temperature dependence of the Seebeck coefficient described by the equation $S = \frac{3}{2} \frac{k_B}{q_e} \ln T + C$, where C depends on the concentration and effective mass of charge carriers, as well as on the Debye temperature. This dependence has the same character as dependence σS² – T and have maximum around 1100K.

*Corresponding author: Email: irklinakhutsrishvili52@gmail.com;

Additionally, the dependences of power factor on specific electrical conductivity were studied. For different thermoelectrics they are described by empirical expressions such as $\sigma S^2 \cong (a/\sigma)^b$ or $\sigma S^2 \cong c\sigma^{-d}$, where constants a, b, c and $d > 0$. For a number of thermoelectrics, the dependences σS^2 on the Seebeck coefficient are rectilinear, while for another series they are power-law. And this is a more general case. The temperature dependences of σS^2 and of scaled power factor (B_s) are also studied. Both are described by a quadratic equation. It has been established that the maximum power factor corresponds to the minimum B_s . Thus, in this case to estimate $(\sigma S^2)_{\max}$ can be used as σ_{\min} , and $(B_s)_{\min}$.

Keywords: Thermoelectrics; power factor; electrical conductivity.

1. INTRODUCTION

Since the seventies of the last century, the $\text{Si}_x\text{Ge}_{1-x}$ alloy has been used in thermoelectric generators in spacecraft for long-distance flights with a long service life [1-3]. This alloy is also used in many branches of science and technology [4-15].

N-type $\text{Si}_x\text{Ge}_{1-x}$ has a number of advantages over the P-type: the maximum of figure of merit (ZT) is about 2.5 times greater for N-type than for P-type (at concentration of charge carriers $n = 3.2 \cdot 10^{26} \text{m}^{-3}$ and at the same compositions). This follows from the fact that the specific electrical conductivity is 2.5-3 times higher, Seebeck coefficient is 1.4-2 times larger (accordingly, the power factor is ~2 orders of magnitude greater), and thermal conductivity coefficient is 1.1-1.3 times smaller at the same temperatures. Also with neutron fluencies $\geq 10^{19}$ and irradiation temperatures $\geq 600^\circ\text{C}$ N-type $\text{Si}_x\text{Ge}_{1-x}$ is more radiation resistant [16].

This article is a continuation of work [17], where the maximization of the figure of merit of thermoelectric material SiGe is considered. Together with ZT, power factor (PF) is an important energy characteristic of thermoelectrics, which is included in the expression of the ZT: $\text{PF} \cong \sigma S^2$, where σ is the specific electrical conductivity, S - Seebeck coefficient. Here we consider N- $\text{Si}_x\text{Ge}_{1-x}$ alloy ($x=0.7, 0.72, 0.76, 0.8$ and 0.83) based on experimental data of [18]. Since the remaining thermoelectric materials are also taken from the literature, the experimental section is not included.

2. DISCUSSION

According to a fairly large number of works, the range of changes of the Seebeck coefficient is $(1-4)10^{-4} \text{V/K}$. With such a relatively narrow

range, the $\sigma S^2 - S$ dependence is almost rectilinear: $\sigma S^2 = kS + b$, where k is the slope of the straight lines, and b is the ordinate of the point of their intersection with the axis σS^2 when extrapolating these lines to $S \rightarrow 0$. From the last equation we get: $S = \frac{k}{2\sigma} + \left[\left(\frac{k}{2\sigma} \right)^2 + \frac{b}{\sigma} \right]^{1/2}$. After simple transformations we will have: $\sigma S^2 = \frac{k}{2\sigma} + b$, that is, in this case $(\text{PF})_{\max}$ will correspond to σ_{\min} .

Fig 1 shows $\sigma S^2 - S$ dependencies for different thermoelectric materials, namely for a, b and c. These dependencies are constructed based on experimental data from the following works: [18] (SiGe), [19] $(\text{Bi}_2\text{Sr}_{1.925}[\text{Sr}(\text{BO}_2)_2]_{0.075}\text{Co}_{1.8}\text{O}_y)$, $\text{Bi}_2\text{Sr}_2\text{Co}_{1.8}\text{O}_y$, [20] $(\text{SiGeMo}_{0.2})$, and [21] $(\text{Sb}_{1.7}\text{Bi}_{0.4}\text{Te}_3)$.

Fig 2 shows $\lg(\sigma S^2)_{\max} - \lg\sigma_{\min}$ dependences for different thermoelectrics using literature and our data. In the obtained intervals of change of variables, these dependencies can be described as a whole by the empirical expression $\lg(\sigma S^2)_{\max} \cong 0.583(\lg\sigma_{\min})^2 - 3.332\lg\sigma_{\min}$ (solid line in Fig.2). The entire dependence is divided into three areas: (I) $10^{-2} < (\text{PF})_{\max} < 10^{-3}$, (II) $10^{-3} < (\text{PF})_{\max} < 10^{-4}$ and (III) $10^{-4} < (\text{PF})_{\max} < 10^{-5} \text{W/K}^2\text{m}$. By means of this approximate relationship, it will be possible to predict the order of $(\text{PF})_{\max}$ according to σ_{\min} . The scatter of points around the averaged line is apparently due to the non-strict rectilinearity of the corresponding $\sigma S^2 - S$ dependences. When these dependencies are practically rectilinear, then the points fit well on the curve (compare Figs.1 and 2).

Fig 3 shows the temperature dependences of $\sigma S^2 - T$ and $S - \ln T$ for $\text{Si}_{0.72}\text{Ge}_{0.28}$ and $\text{Si}_{0.76}\text{Ge}_{0.24}$ (dependencies for other compositions have the same form). From this figure it is clear that these dependences have a maximum at the same temperature ($\sim 1100\text{K}$).

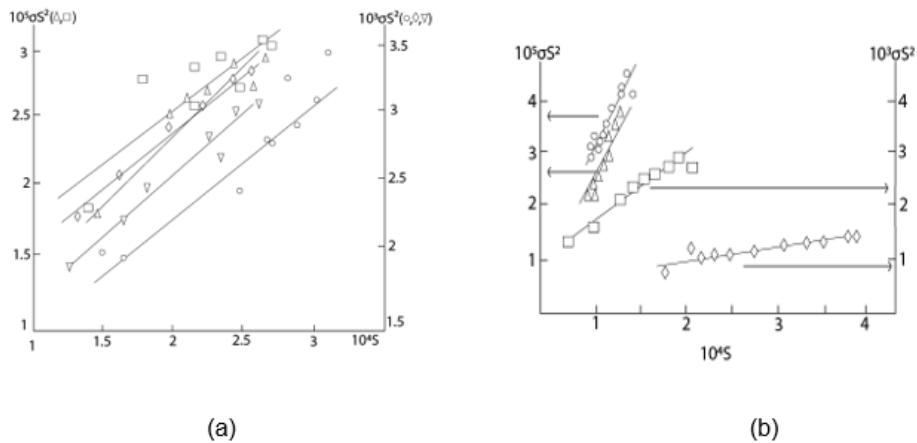


Fig. 1. Typical dependences $\sigma S^2 - S$: (a) $\text{Si}_x\text{Ge}_{1-x}$, $x=0.7$ (o), 0.72 (Δ), 0.76 (\square), 0.8 (\diamond) and 0.83 (∇); (b) (o) $\text{Bi}_2\text{Sr}_{1.925}[\text{Sr}(\text{BO}_2)_2]_{0.075}\text{Co}_{1.8}\text{O}_y$, (Δ) $\text{Bi}_2\text{Sr}_2\text{Co}_{1.8}\text{O}_y$, \square - $\text{SiGeMo}_{0.2}$, and (\diamond) $\text{Sb}_{1.7}\text{Bi}_{0.4}\text{Te}_3$. $[\sigma S^2]=\text{W/K}^2\text{m}$, $[S]=\text{V/K}$

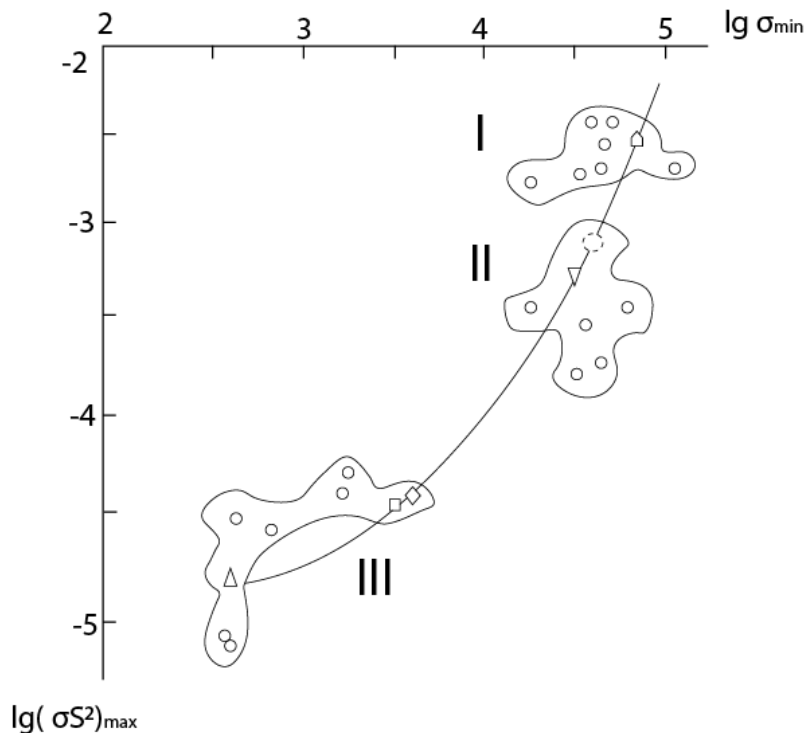


Fig. 2. Dependences $\lg(\sigma S^2)_{\max} - \lg\sigma_{\min}$. The coordinates of the points are calculated according to the data of following works: sect.I - [18] ($\text{Si}_{0.7}\text{Ge}_{0.3}$), [20] (SiGe , $\text{SiGeMo}_{0.2}$), PbTe [22]; sect.II - [21] ($\text{Sb}_{1.7}\text{Bi}_{0.4}\text{Te}_3$), [23] Bi_2Te_3 , $(\text{Bi}_{0.98}\text{Sn}_{0.02})_2\text{Te}_{2.7}\text{Se}_{0.3}$, [24] $\text{Si}_{0.68}\text{Ge}_{0.32}\text{Ga}$, [25] Ni_2CuCrFe ; sect.III - [19] $\text{Bi}_2\text{Sr}_2\text{Co}_{1.8}\text{O}_y$, $\text{Bi}_2\text{Sr}_{1.9}[\text{Sr}(\text{BO}_2)_2]_{0.1}\text{Co}_{1.8}\text{O}_y$ (and the same thermoelectrics with different composition of components). Figurative points correspond to Fig.1: Δ - $\text{Bi}_2\text{Sr}_2\text{Co}_{1.8}\text{O}_y$, \square - $\text{Si}_{0.72}\text{Ge}_{0.28}$, \diamond - Bi_2Te_3 , ∇ , \circ - SiGeGa , \triangle - $\text{SiGeMo}_{0.2}$

It should be noted that for practically all other thermoelectrics considered above (and also for $\text{P-Si}_x\text{Ge}_{1-x}$), a rectilinear dependence of the Seebeck coefficient on the natural logarithm of

temperature was observed (Fig.3). Therefore, for them the following formula was used [25,26]:

$$S = \frac{3}{2} \frac{k_B}{q_e} \ln T + C, \quad (1)$$

where C depends on the concentration and effective mass of charge carriers, as well as on the Debye temperature (k_B - Boltzmann's constant, q_e - elementary charge, T - absolute temperature)^(*). Fig 3(b) shows these dependences for $Sb_{1.7}Bi_{0.4}Te_3$, $Tl_9Sb_{0.99}Sn_{0.1}Te_6$ [27] and $SiGeMo_{0.2}$. From Fig.4(a) it is clear that the experimental points form a

practically single set with an average overall slope $K \equiv tg\alpha \cong 1.122 \cdot 10^{-4}$. The slopes of the lines presented in Fig.3(b) are $tg\alpha \cong 1.324$, 1.475 and $1.050 \cdot 10^{-4}$, respectively. These slopes which approach to $K = \frac{3 k_B}{2 q_e} \cong 1.293 \cdot 10^{-4}$ with more or less accuracy.

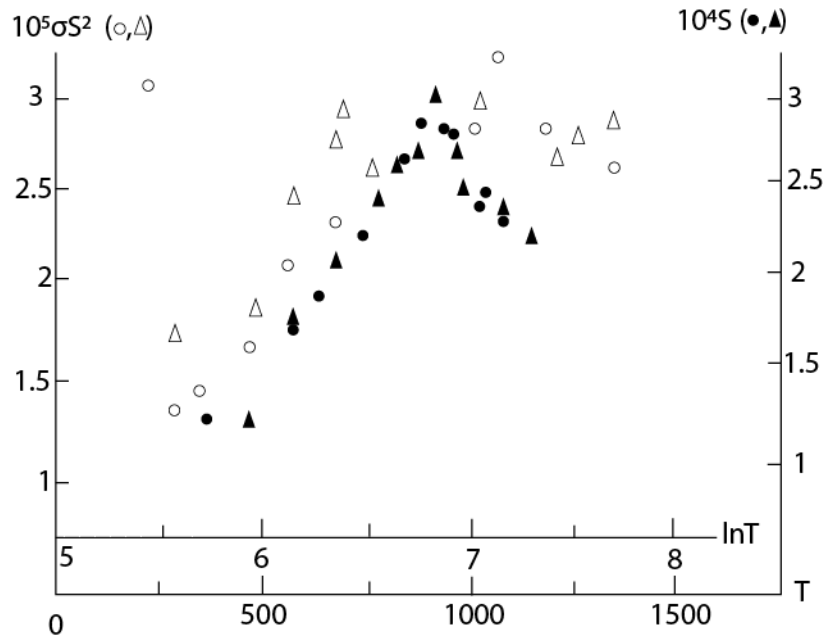


Fig. 3. Dependencies $\sigma S^2 - T$ and $S - \ln T$ for $Si_{0.72}Ge_{0.28}$ (o, Δ) and $Si_{0.76}Ge_{0.24}$ (•, \blacktriangle). ($\ln 1100 \cong 7$, the scales are different on the abscissa axes) [σS^2]=W/K²m, [S]=V/K, [T]=K

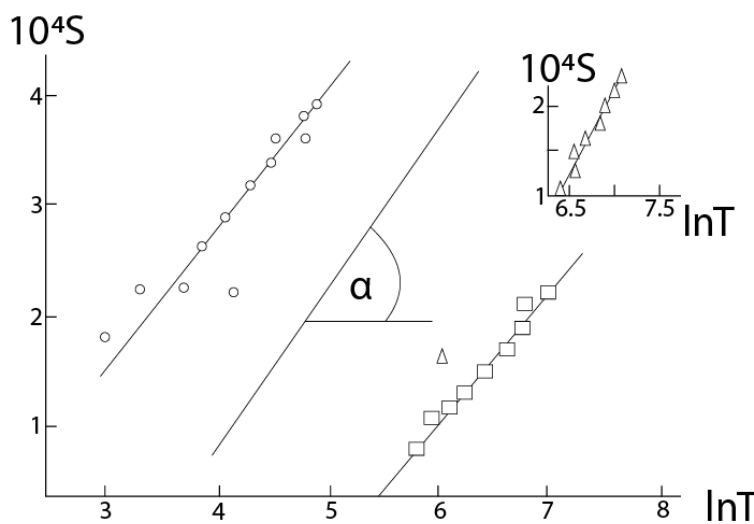


Fig. 4. Dependences $S - \ln T$ for $Sb_{1.7}Bi_{0.4}Te_3$ (o), $Tl_9Sb_{0.99}Sn_{0.1}Te_6$ (Δ) and $SiGeMo_{0.2}$ (\square). A straight line without points was constructed at $tg\alpha \cong 1.293 \cdot 10^{-4}$ with arbitrarily taken $b = -4.4$. [S]=V/K, [T]=K

Since the values of K do not coincide exactly with $\frac{3}{2} \frac{k_B}{q_e}$, it is difficult to estimate the corresponding values of the constant A (see Footnote below) from the values of C calculated below. However, according to as yet unpublished data for P-Si_{0.7}Ge_{0.3}, the temperature dependence of mobility is described by the expression $\mu \cong \frac{1}{2} T^{-3/2}$, which indicates phonon scattering of charge carriers [28].

NOTE

(*) $C = \frac{k_B}{q_e} \left[A + \ln \frac{2(2\pi m^* k_B)^{3/2}}{(2\pi h^3)^3 n} \right]$, where A depends on the scattering mechanism and takes values from 2 to 4 (m^* and n – effective mass and concentration of charge carriers).

3. CONCLUSION

A method is proposed for determining the maximum power factor of Si_xGe_{1-x} alloys of different compositions and different conductivities. Other thermoelectrics are also considered based on literature data.

The dependences $\lg(\sigma S^2)_{\max} - \lg\sigma_{\min}$ for various thermoelectrics based on literature and our data in the corresponding interval of changes of variables are described by a one empirical expression $\lg(\sigma S^2)_{\max} \cong 0.583(\lg\sigma_{\min})^2 - 3.332\lg\sigma_{\min}$.

The temperature dependence of the Seebeck coefficient described by the equation $S = \frac{3}{2} \frac{k_B}{q_e} \ln T + C$. This dependence has the same character as dependence $\sigma S^2 - T$ and have maximums around 1100K.

COMPETING INTERESTS

Authors have declared that no competing interests exist.

REFERENCES

1. Yang J, Caillat T. Thermoelectric materials for space and automotive power generation. *MRS Bulletin*. 2006;31(3): 224-229.
2. Ayachi S, X He, Yoon HJ. Solar thermoelectricity for power generation. *Advanced Energy Materials*. 2023;13(28): 2300937.
3. Angelo M.d', Galassi C, Lecis N. Thermoelectric materials and applications: A review. *Energies*. 2023;16(17):6409.
4. Basu R, Singh A. High temperature Si–Ge alloy towards thermoelectric applications. *Materials Today Phys*. 2021;21:100468.
5. Cook B. Silicon–Germanium: The legacy lives on. *Energ*. 2022;15: 2957.
6. Schwinge C, Kühne K, Emara J et al. Optimization of LPCVD phosphorous-doped SiGe thin films for CMOS-compatible thermoelectric applications. *Appl. Phys. Lett*. 2022;120:031903.
7. Big-Alabo A. Finite element modelling and optimization of Ge/SiGe super lattice based thermoelectric generators. *Appl. Sci*. 2021;3:189.
8. Jang K, Kim Y, Park J. et al. Electrical and structural characteristics of excimer laser-crystallized polycrystalline Si_{1-x}Ge_x thin-film transistors. *Materials*. 2019;12:1739.
9. Murata H., Nozawa K., Suzuki T. et al. Si_{1-x}Ge_x anode synthesis on plastic films for flexible rechargeable batteries. *Sci. Report*. 2022;12:13779.
10. Idda A, Ayat L, Dahbi N. Improving the performance of hydrogenated amorphous silicon solar cell using a-SiGe:H alloy. *Ovonic Res*. 2019;15:271–278.
11. Singh A.K., Kumar M., Kumar D. et al. Heterostructure silicon and germanium alloy based thin film solar cell efficiency analysis. *Engin. and Manufacturing*. 2020; 2:29–40.
12. Zimmerman H. SiGe photodetectors, in *Silicon Optoelectronic Integrated Circuits*, eds. K.Chun, K.Itoh, T.H.Lee et al. Vienna, Austria. 2018:1-435.
13. Aberl J, Brehm M, Fromherz J. et al. SiGe quantum well infrared photo detectors on strained-silicon-on-insulator. *Opt. Express*. 2019;27:32009–32018.
14. Koumoto K, Terasaki I, Funahashi R. Complex oxide materials for potential thermoelectric applications. *MRS Bull*. 2006;31:206-210.
15. Ellis BL, Nazar LF. Sodium and sodium-ion energy storage batteries. *Current Opinion Solid State and Materials Sci*. 2022;16:168-177.
16. Bokuchava G. Physical-mechanical and electrophysical properties of polycrystalline silicon- germanium alloys. Thesis, Tbilisi. 2008:1-135.
17. Nakhutsrishvili I, Adamia Z, Kakhniashvili G. Maximization of figure of merit of alloy Si_xGe_{1-x}. *Materials Sci. Res. and Rev*. 2023;6:918-922.

18. Barbakadze K, Bokuchava G, Isakadze Z. et al. High temperature thermoelectric generator based on SiGe alloy. *Sci. J. LEPL – Agmashenebeli Nat. Defence Acad. of Georgia.* 2022;47-50.
19. Kuzanyan A, Margiani N, Zhghamadze V. et al. Effect of $\text{Sr}(\text{BO}_2)_2$ dopant on the power factor of $\text{Bi}_2\text{Sr}_2\text{Co}_{1.8}\text{O}_y$ thermoelectric. *Contemporary Phys.* 2021; 56:146-249.
20. Li Y, Han J, Xiang Q. et al. Enhancing thermoelectric properties of p-type SiGe by SiMo addition. *Materials Sci.: Mater. Electron.* 2019;30:9163-9170.
21. Scheele M, Oeschler N, Veremchuk I. et al. ZT enhancement in solution-grown $\text{Sb}_{2-x}\text{Bi}_x\text{Te}_{3-2x}$ nanoplatelets. *ASC Nano.* 2010; 4:4283-4291.
22. Sauerschnig P, Jood P, Ohta M. Improved high-temperature material stability and mechanical properties while maintaining a high figure of merit in nanostructured p-type PbTe-based thermoelectric elements. *Adv. Materials Technol.* 2023;8:2201295.
23. Hedge GCh., Prabhu AN, Chattopadhyay MK. Improved electrical conductivity and power factor in Sn and Se co-doped melt-grown Bi_2Te_3 single crystal. *Mater. Sci.: Mater. Electron.* 2021;32:24871-24888.
24. Omprakash M, Arivanandhan M, Koyama T. et al. High power factor of Ga-doped compositionally homogeneous $\text{Si}_{0.68}\text{Ge}_{0.32}$ bulk crystal grown by the vertical temperature gradient freezing method. *Cryst. Growth & Design* 2015;15:1380-1388.
25. Kush L., Srivastava S, Jaiswal Y. and Srivastava Y. Thermoelectric behaviour with high lattice thermal conductivity of Nickel base $\text{Ni}_2\text{CuCrFeAl}_x$ ($x = 0.5, 1.0, 1.5$ and 2.5) high entropy alloys. *Materials Resh. Expr.* 2020;7:035704.
26. Tewari GC, Tripathi TS, Yamauchi H, Karppinen M. Thermoelectric properties of layered antiferromagnetic CuCrSe_2 . *Materials Chem. and Phys.* 2014;145:156-161.
27. Tanaka Y. Metal complex molecular junctions as thermoelectric devices. *Chem. Europe.* 2023;29:e202300472.
28. Alfaramavi K, Alzamil MA. Temperature-dependent scattering processes of n-type indium antimonide. *Optoelectr. Adv. Mater.- Rapid Communicat.* 2009;3:569-573.
29. Khan WM, Shah WH, Khan N. et al. Effects on the seebeck co-efficient and electrical properties of $\text{Tl}_{10-x}\text{ATe}_6$ ($A = \text{Pb} \& \text{Sn}$) in chalcogenide system. *Ovonic Res.* 2021;17:201.

© Copyright (2024): Author(s). The licensee is the journal publisher. This is an Open Access article distributed under the terms of the Creative Commons Attribution License (<http://creativecommons.org/licenses/by/4.0>), which permits unrestricted use, distribution, and reproduction in any medium, provided the original work is properly cited.

Peer-review history:

The peer review history for this paper can be accessed here:
<https://www.sdiarticle5.com/review-history/116184>